Quantitative Study of the Ionization-Induced Refraction of Picosecond Laser Pulses in Gas-Jet Targets

A. J. Mackinnon,[1] M. Borghesi,[1] A. Iwase,[1] M. W. Jones,[1] G. J. Pert,[2] S. Rae,[3] K. Burnett,[3] and O. Willi[1]
[1]*The Blackett Laboratory, Imperial College of Science, Technology and Medicine, London SW7 2BZ, United Kingdom*
[2]*University of York, Heslington, York, United Kingdom*
[3]*Clarendon Laboratory, Oxford University, Oxford, United Kingdom*
(Received 20 November 1995)

A quantitative study of refractive whole beam defocusing and small scale breakup induced by optical ionization of subpicosecond and picosecond, 0.25 and 1 μm, laser pulses in gas-jet targets at densities above 1×10^{19} cm^{-3} has been carried out. A significant reduction of the incident laser intensity was observed due to refraction from ionization-induced density gradients. The level of refraction measured with optical probing correlated well with the fraction of energy transmitted through the plasma. The numerical and analytical models were found to agree well with experimental observations.

PACS numbers: 52.50.Jm, 32.80.Rm, 52.35.Tc

The interaction of ultrashort high power laser pulses with gaseous and plasma targets has applications in x-ray laser, high harmonic generation, particle acceleration, and fast igniter studies [1–3]. In general, for these applications irradiances exceeding 10^{18} W cm^{-2} are required. Refractive defocusing of short laser pulses, however, may limit the irradiances which can be achieved. In particular, refraction effects may be important when dense gaseous targets are used where large density gradients are generated due to rapid ionization. This problem may affect the propagation of laser pulses through the gas filled hohlraums that have been proposed for inertial confinement fusion applications. The subject of defocusing has been studied theoretically [4], where an estimate of the characteristic defocusing length was obtained. Recently, more detailed treatments of refraction have been published including an analytic model that predicted the maximum achievable intensity and ionization stage as a function of the gas, density, and focusing optics [5]. Numerical solutions to the wave equation in the paraxial approximation [6] also confirmed that defocusing clamped the incident intensity. Experimental studies of ionization-induced defocusing have been carried out in gas cells [7], where an empirical relation was found between the focused intensity and gas cell pressure. Applications such as recombination x-ray lasers require highly uniform ionized plasma channels of high density extending over several millimeters for high gain and energy efficiency [1]. It may, however, be difficult to achieve such conditions in high density gaseous targets due to whole beam refraction and small scale breakup of laser inhomogeneities. An understanding of the limits placed on the plasma length and ionization stage achieved in gas-jet targets due to refraction is essential to determine their feasibility for x-ray laser and other applications.

This Letter presents space resolved measurements of the initial plasma density profiles and plasma uniformity obtained during two separate experiments with similar gas-jet targets at high density. In the first experiment a 1 to 3 ps, 1.054 μm laser pulse was focused at a vacuum intensity up to 3×10^{18} W cm^{-2} onto the edge of a helium or neon gas jet. In the second a 350 fs, KrF laser pulse was focused at a vacuum intensity up to 6×10^{16} W cm^{-2} into the middle of a similar jet. For both experiments the refractive defocusing was measured as a function of gas density using optical probing. These observations were consistent with measurements of the transmitted laser energy. Simulations agreed with the refraction observed, and the reduction of the focused laser intensity in the plasma was inferred from numerical models.

The experiments were performed on different laser systems at the Rutherford Appleton Laboratory. The first experiment was carried out on the VULCAN Nd:glass laser operating in the chirped pulse amplifications mode (CPA) [8] with the compression gratings located under vacuum in the target chamber. An $F/5$ off axis parabola focused the beam onto the gas vacuum boundary with a typical focal spot of 30 μm full width at half maximum (FWHM). The nominal vacuum intensity (I_v) was (1–3) $\times 10^{18}$ W cm^{-2} with a 200 ps prepulse (FWHM) at an intensity of 10^{13} W cm^{-2}. The second series of experiments was undertaken on the SPRITE KrF laser. The laser was also operated in CPA mode. The pulse length was 350 fs (FWHM), with an energy of 150–300 mJ on target. The laser pulse was focused onto the middle of the gas-jet target with a focal spot of 30 μm (FWHM) by an $F/4.5$ off axis parabolic mirror giving $I_v = 6 \times 10^{16}$ W cm^{-2}. The main pulse was superimposed on a 20 ns (FWHM) amplified spontaneous emission pulse at an irradiance of 1×10^{9} W cm^{-2}. For both experiments a solenoid pulsed gas-jet target was used with a 1 mm diameter cylindrical nozzle. The gas flow was subsonic, resulting in a gas density gradient along the laser propagation direction, which typically gave a factor of 3 reduction in gas density from center out to a radius of 500 μm. Both neon and helium gases were used with a neutral gas density over the range

0031-9007/96/76(9)/1473(4)$06.00

1×10^{19}–$1.5 \times 10^{20} \pm 10\%$ cm^{-3}. In both experiments the plasma was diagnosed with a temporally independent probe pulse which was split off the main uncompressed heating beam. On VULCAN, the split-off was compressed on a pair of gratings and frequency doubled in a KDP crystal resulting in a probe wavelength of 0.527 μm and a pulse duration of a few picoseconds. On SPRITE the uncompressed KrF pulse with a duration of less than 10 ps was used. A moiré deflectometer [9] probed the electron density gradient and density profiles at discrete intervals for times up to 2 ns after the end of the pulse. The optical system gave a resolution of 1 μm, however, diffractive effects from the moiré gratings limited the fringe resolution to 7 μm in the transverse direction. Calorimetry of the laser energy transmitted through the target within an acceptance angle of 5.5 deg was also used.

A number of numerical models were used for data interpretation, for detailed comparison with experimental measurements and the analytical theory. A numerical 2D wave propagation code was used to model the interaction [6]. This solved the paraxial wave equation numerically in cylindrical symmetry for a transverse electric field of the form $E = u(r, z, t) \exp[i(kz - \omega t)]$, where r and z are the radial and longitudinal coordinates, respectively. The free electron contribution to the refractive index was calculated at each grid point using the tunnel ionization model [10], which was limited to include ionization up to the third stage only. The initial laser profile was assumed to be Gaussian and the output from the code was in the form of 2D intensity and density contours of the radial distribution of the laser intensity for the laser pulse and the total electron density throughout the gas jet. The electron temperature was predicted using an inverse bremsstrahlung model that contained a correction to the electron collision frequency at high laser fields, due to the inability of the plasma to shield the high frequency quiver oscillations of the electrons. This increased the upper limit of the maximum impact parameter in the Coulomb logarithm term from the Debye length to the excursion distance of the electron in the laser field [11]. Under these conditions the Langdon effect [12] was not important and was not included in the model. The expansion characteristics of the plasma following the laser heating stage were modeled using the MEDUSA code. The plasma temperature was inferred by fitting the temporal evolution of the plasma radius predicted by the simulation to the experimentally measured expansion characteristics, using the initial energy of the plasma as the adjustable parameter, as described in detail in a previous publications [13].

A moiré deflectogram of the plasma taken 6 ps after focusing a 2.8 ps, 16 J, 1.05 μm laser pulse at a vacuum intensity of 8×10^{17} W cm^{-2} onto the edge of the gas jet is shown in Fig. 1(a). The vacuum focusing position is at the right hand edge of the field of view and the gas density increases from 1×10^{19} to 3×10^{19} cm^{-3} ($\pm 5 \times 10^{18}$ cm^{-3}) from the edge to the center as shown in Fig. 1(c). In Figs. 1(a) and 1(b) the plasma radius

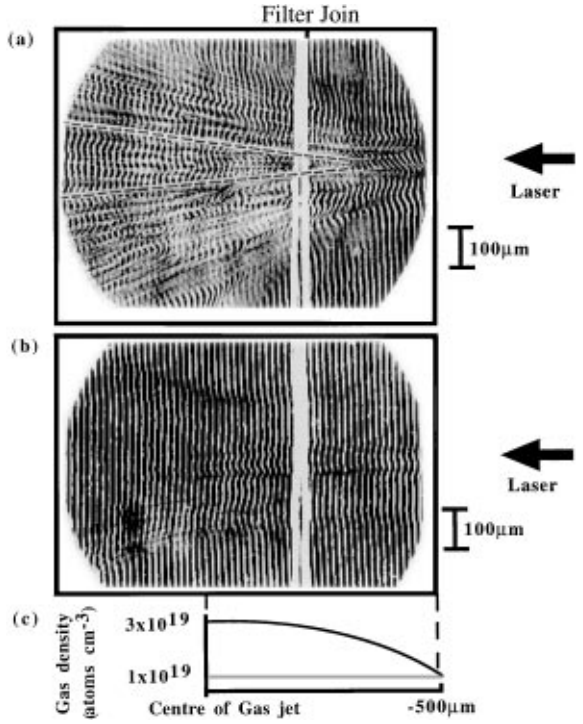

FIG. 1. Moiré deflectograms of expanding plasma 6 ps after focusing 5 TW, 1 μm laser pulses on the vacuum-gas boundary for (a) neon and (b) helium, both at a center density of 3×10^{19} cm^{-3}. The vertical bar near the center of the picture is an imperfection of the filters in front of the film. The laser is incident from the right and the expansion of the beam at 5.7 deg due to the focusing optics is superimposed on (a). The gas density gradient variation along the gas jet is shown in (c).

can be seen to increase with a characteristic angle much greater than the 5.6 deg cone angle of the $F/5$ focusing optics, which is superimposed on the figure. The plasma also broke up into a number of ionization channels which split further as the laser propagated through the jet. The electron density measured by the deflectrometer at the vacuum focusing position was 4×10^{19} cm^{-3}, giving an ionization stage, Z^*, of 4^+, this is lower than the value of 8^+ expected from the Coulomb barrier model [14] if the vacuum laser intensity of 8×10^{17} W cm^{-2} was used. This was because the gas extended 200 μm before the vacuum focusing position, causing significant refraction of the beam before it reached best focus. For these conditions the plasma was strongly refractive with a characteristic defocusing length, length, l_d, of 14 μm, where $l_d = \lambda/2 (n_{\rm cr}/n_e)$, λ is the laser wavelength, $n_{\rm cr}$ and n_e are the critical electron and electron density, respectively [4]. The refraction angle α after a propagation length of 800 μm (the extent of the field of view of Fig. 1) was measured from Fig. 1(a) to be 23 deg. By assuming negligible energy depletion due to absorption, the fraction of the incident laser energy that was transmitted into the 5.5 deg acceptance angle of the calorimeter, as compared to the vacuum case, was used to calculate the expansion angle of the beam. For Fig. 1(a) the transmission fraction was

2.5%, corresponding to a beam expanding at 30 deg. These observations compared well with a simple estimate of α caused by the density gradient across the focal spot, obtained from the refraction formula, $\alpha(\text{degrees}) \sim 2.23 \times 10^{-12} \lambda^2 (dn_e/dx) dL$ [15], where λ is the laser wavelength, dn_e/dx is the transverse electron density gradient, and dL is the plasma path length (both in cgs units). For an average electron density $n_e = 4 \times 10^{19}$ cm^{-3}, $dL = 800 \times 10^{-4}$ cm, $dx = 3 \times 10^{-4}$ cm, and $\alpha = 26$ deg. In contrast for helium at the same gas density, $\alpha = 17$ deg from Fig. 1(b) and the measured 14% energy transmission fraction corresponded to a beam expanding at 14 deg. This was entirely consistent with the value of 13 deg obtained from the refraction formula at the lower electron density of 2.0×10^{19} cm^{-3}, measured at the vacuum focusing position. In general, as the gas density was increased the observed refraction angle increased and both the transmitted laser energy and length of ionized plasma were reduced. The observed refraction angle and the measured transmitted laser energy (within the 5.5 deg calorimeter acceptance angle) as a function of neon gas density is plotted in Fig. 2. The observed angle increased from 23 to 40 deg when the gas density was increased from 3×10^{19} to 9×10^{19} cm^{-3}, while the fraction of laser energy transmitted reduced from 2.5 to less than 1%.

A simple scaling law relating the average intensity $I(L)$ in the plasma to the density gradient and propagation length L was determined from the above results. The radius of the beam, r, as a function of L was extracted from the refraction angle, $r = \{L \tan(\alpha)$ and if, as a first approximation, the laser spot was assumed to be a top hat function then $I(L) = P/\pi[L \tan(\alpha)]\}^2$, where $P(W)$ is the total laser power in watts. Inserting α from the refraction formula gives $I(L) = P/\pi\{L \tan[(2.23 \times 10^{-12})\lambda^2 (dn_e/dr) L]\}^2$, with n_e, L, and r all in units of cm. For the case in Fig. 1(a), at $L = 800$ μm, $I \sim 1 \times 10^{15}$ W cm^{-2}, which is only just above threshold for 1^+ neon [14] this agreed well with the small fringe shifts observed in Fig. 1(a) at $L = 800$ μm.

The effect of refraction when the laser was focused into the middle of the gas jet was also studied in a separate experiment with a 0.248 μm, 350 fs pulse at a vacuum intensity up to 6×10^{16} W cm^{-2}. In this experiment the radius of the plasma was found to increase as the gas density increased, the point of maximum density was shifted from the center of the gas jet towards the laser, and the plasma again broke up into numerous channels which split and refracted away from the propagation axis. The ionization channels observed in Fig. 1(a) and in the 0.248 μm experiment were not thought to arise from any filamentation mechanism but from refractive splitting of hot spots in the laser beam. The distance taken for the channels to split was approximately estimated from a ray propagation argument [16]. For a hot spot of radius a, the density gradient across the channel of dn_e/da due to the ionization will refract the laser and cause the channel to split within a distance of $dz \sim da(n_{\text{cr}}/2n_e)^{1/2}$ [16]. For the 0.248 μm laser, assuming neon 1^+ at an electron density n_e of 1.5×10^{20} cm^{-3}, $n_e/2n_{\text{cr}} = 4 \times 10^{-3}$, and for hot spots of radius 10 μm, $da = 10$ μm, then $dz = 77$ μm. This agreed well with the splitting distance of 100 ± 50 μm observed experimentally under these conditions. If the intensity was high enough to cause the electrons to oscillate relativistically then self-focusing could cause the observed plasma nonuniformity. The threshold for this is given by $P_{\text{cr}} = 17(n_{\text{cr}}/n_e)$ GW [17]. For the 0.248 μm experiment, $P_{\text{cr}} = 2$ TW, whereas channels first appeared at an average power below 100 GW, relativistic filamentation was therefore discounted.

Images of the distribution of light refracted through the plasma were obtained by imaging the focal spot region with an $F/2.5$ quartz lens. It was found that as the gas density increased from zero to 1×10^{20} cm^{-3} the width of the laser focal spot increased from 17 to >100 μm. This corresponded to a lowering of the laser intensity from 2×10^{17} to 3×10^{15} W cm^{-2}, confirming that the refractive defocusing limited the focused intensity. The experimental results for the case of focusing in the center of the jet were compared with the analytical and numerical defocusing models. The maximum intensities predicted by the analytical model [5] were

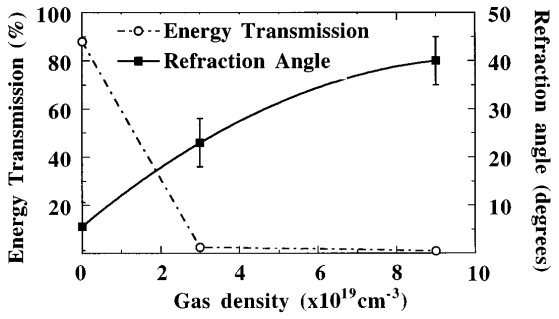

FIG. 2. The correlation of the observed plasma refraction angle and the laser energy transmission fraction (within the 5.5 deg acceptance angle of the calorimeter) versus gas density for neon.

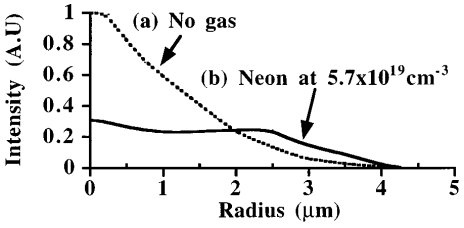

FIG. 3. Numerical model results showing intensity profiles for a 350 fs, 0.248 μm laser pulse at a vacuum intensity of 5×10^{16} W cm^{-2}, with (a) vacuum and (b) neon gas at a density of 5.7×10^{19} cm^{-3}. The profile in (a) is of a diffraction limited Gaussian, while (b) shows the light refracted away from the laser axis. The peak laser intensity near the gas-jet center in (b) is reduced to 1.2×10^{16} W cm^{-2} by the refractive defocusing effect.

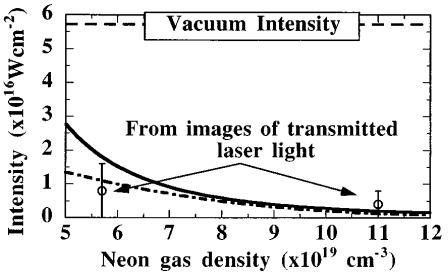

FIG. 4. Variation of intensity with density for the 0.248 μm experiment and models, at a vacuum intensity of $6 \times 10^{16}\,\mathrm{W\,cm^{-2}}$. The results of the analytical model derived by Fill [5] (full curve) and the numerical model of Rae [6] (dashed curve) are compared to the experimental points obtained from images of the transmitted laser light.

1.8×10^{16} and $8 \times 10^{14}\,\mathrm{W\,cm^{-2}}$ for a laser focused with $F/4.5$ optics into neon at gas densities of 5×10^{19} and $1.5 \times 10^{20}\ \mathrm{cm^{-3}}$, respectively. The importance of refraction of the laser light was confirmed with 2D numerical simulations, which were carried out for a 350 fs, 0.25 μm pulse at a vacuum intensity of $5 \times 10^{16}\,\mathrm{W\,cm^{-2}}$. A cross section through the peak intensity of the laser pulse in the numerical simulation both without and with gas are shown in Figs. 3(a) and 3(b), respectively. Figure 3(a) shows a Gaussian peaked on axis with a half width at half maximum (HWHM) around 1.5 μm, consistent with the diffraction limit for a KrF beam focused with the $F/5$ lens used in the simulation. In contrast, for a gas density of $5.7 \times 10^{19}\ \mathrm{cm^{-3}}$ the simulated density profile shown in Fig. 3(b) demonstrates that the laser light is refracted from the axial density gradients, increasing the spot radius by a factor of 2 and lowering the peak intensity by a factor of 4. The maximum laser intensity predicted by the numerical model was $1.2 \times 10^{16}\,\mathrm{W\,cm^{-2}}$ for $5.7 \times 10^{19}\,\mathrm{cm^{-3}}$ neon and $3 \times 10^{15}\,\mathrm{W\,cm^{-2}}$ for $1.8 \times 10^{20}\ \mathrm{cm^{-3}}$, which agreed within a factor of 2 with the analytical model. A graph that summarizes the maximum focused intensity as a function of gas density predicted by the models and the experimental measurements (obtained by fitting a Gaussian to the images of the transmitted laser light) is shown in Fig. 4. Both the numerical and analytical models agreed within a factor of 2 of the experimental data. The reduction of the focused intensity was also confirmed by comparing the electron temperature measured from the rate of plasma expansion with that predicted by the adsorption model [11]. For neon at $5 \times 10^{19}\ \mathrm{cm^{-3}}$ with a vacuum intensity of $5 \times 10^{16}\,\mathrm{W\,cm^{-2}}$ the measured electron temperature was 80 ± 20 eV. Under these conditions the absorption models predicted an electron temperature of 282 eV, and agreement between the model and data could only be obtained if the incident intensity was reduced from 5×10^{16} to $9 \times 10^{15}\,\mathrm{W\,cm^{-2}}$. Such a temperature reduction was caused by the decrease in Z^* due to the lower laser intensity.

In conclusion, the limitation of intensity in interactions of intense laser beams with gas-jet targets has been observed. When the laser was focused into the middle of the gas jet the intensity was limited by refraction and gave essentially the same result as focusing into a gas cell. When the 1 μm laser was focused onto the edge of the jet the observed angle of refraction was significantly greater than the diffraction limited divergence. It was also consistent with the transmitted laser energy measured by the calorimeter and with the refraction angle determined from the measured electron densities. The refractive defocusing was observed to be more severe at 1 μm than 0.25 μm, in accordance with the λ^2 scaling of the refraction angle with wavelength. A simple expression allowed the laser intensity to be predicted as a function of the propagation distance, electron density gradient, and laser wavelength. A strong feature of both experiments was the formation of ionization channels which split as the laser propagated, these were consistent with refractive splitting of laser hot spots. Finally, the most promising solution to the refraction problem would use preformed plasmas [4,18] to maintain long interaction lengths at high laser intensities and densities.

The authors would like to acknowledge the contributions made by the staff of the Central Laser Facility. This work was funded by ESPRC/MoD grant.

[1] D. C. Eder, P. A. Amendt, and S. C. Wilks, Phys. Rev. A **45**, 6761 (1992).
[2] P. Sprangle and E. Esarey, Phys. Fluids B **4**, 2241 (1992).
[3] M. Tobak *et al.*, Phys. Plasmas **1**, 1621 (1994).
[4] R. Rankin *et al.*, Opt. Lett. **16**, 835 (1991).
[5] E. E. Fill, J. Opt. Soc. Am. B **11**, 2241 (1994).
[6] S. C. Rae, Opt. Commun. **97**, 25 (1993).
[7] P. Monot *et al.*, J. Opt. Soc. Am. B **9**, 1579 (1992).
[8] P. Maine *et al.*, IEEE J. Quantum Electron. **24**, 398 (1988).
[9] O. Kafri, Opt. Lett. **5**, 555 (1980).
[10] M. V. Ammosov, N. B. Delone, and V. P. Krainov, Zh. Eksp. Teor. Fiz. **91**, 2008 (1986) [Sov. Phys. JETP **64**, 1191 (1987)].
[11] G. J. Pert, Phys. Rev. E **51**, 4778 (1995).
[12] A. B. Langdon, Phys. Rev. Lett. **44**, 575 (1980).
[13] M. Dunne *et al.*, Phys. Rev. Lett. **72**, 1024 (1994).
[14] S. August *et al.*, Phys. Rev. Lett. **63**, 2212 (1989).
[15] F. C. Jahoda and G. A. Sawyer, in *Methods of Experimental Physics*, vol. 9B (Academic, New York, 1971), Vol. 9B, p. 1.
[16] J. Denavit and D. W. Phillion, Phys. Plasmas **1**, 1971 (1994).
[17] C. Max, J. Arons, and A. B. Langdon, Phys. Rev. Lett. **33**, 209 (1970).
[18] C. G. Durfee III and H. M. Milchberg, Phys. Rev. Lett. **71**, 2409 (1993); A. J. MacKinnon *et al.*, Annual Report to the Central Laser Facility, No. RAL-TR-95-025, 33-36, 1995 (unpublished).